# Development of a Hybrid Solar/UV Lamp Illuminated Annular Photocatalytic Reactor for the Treatment of Distillery Wastewater

John Kabuba

***Abstract*—**In this work, a hybrid solar/UV lamp illuminated annular photocatalytic reactor was developed for the treatment of phenol wastewater. The local volumetric rate of energy absorption (LVREA) in the reactor was evaluated using the. Monte Carlo method from which reaction parameters and the local reaction rate (LRR) were determined. The reaction order with respect to the volumetric rate of energy absorption (VREA) was found to be 0.74 and 0.75 under solar and UV lamp illumination, respectively. A good fit between experimental and simulated reaction rate in the hybrid light reactor was obtained without any adjustable parameters. The LRR distribution in different reactor configurations followed the order: hybrid light > annular UV lamp > annular solar > tubular solar. The optimum catalyst loading with respect to the overall reaction rate was found to be 0.15, 0.2, 0.4 and 0.4 g/L while that with respect to the LRR distribution was 0.01, 0.025, 0.1 and 0.15 g/L for the tubular solar, annular solar, annular UV lamp and hybrid light reactors, respectively. This work highlighted the accuracy of Monte Carlo simulation and the drastic improvement in the LRR distribution due to hybrid light illumination as compared to either solar or UV lamp illumination.

***Keywords*—**Distillery wastewater, Hybrid light, Monte Carlo, Local reaction rate, Photocatalysis

## I. Introduction

TRADITIONALLY, photocatalysis has been carried out using nanophase $TiO_2$ illuminated by mercury ultraviolet (UV) lamps. Most of the reactors used in conventional photocatalysis have been the annular type in which the UV lamp is positioned in the middle of the reactor. The most popular UV lamp for lab scale installations has been the low-pressure black light and germicidal lamps. In such a reactor, most of the light is absorbed in a narrow region near the lamp sleeve which results in poor illumination in the rest of the reactor [1]. The least illuminated region is usually near the reactor wall where the catalysts are poorly illuminated resulting in catalyst wastage and a low reaction rate. To improve the reaction rate and optimize catalyst use, the region near the reactor wall needs to be illuminated. This can be done by employing an external light source such as sunlight. The resulting hybrid light reactor, internally illuminated by the UV lamp and externally illuminated by sunlight, has advantages of good illumination in a compact device. Moreover, the use of free and renewable solar energy significantly reduces the operation cost of the hybrid light reactor. Such a solar/UV lamp hybrid light reactor has been developed for gas phase photocatalysis [2]. A few hybrid light reactors have been reported for wastewater treatment [3, 4]; however, none of these were typical annular reactors. The reactor developed by Durán et al. [4] was essentially a rotating drum reactor consisting of a catalyst coated quartz drum which was internally irradiated by a UVC lamp and externally illuminated by sunlight. Orozco et al. [3] designed a hybrid light reactor made of an acrylic box which was internally irradiated by 6 black light lamps and illuminated by sunlight through a transparent glass at the top of the reactor. Recently, simulation has emerged as a tool of choice for photocatalytic rector design, optimization and scale up [5]. A photocatalytic reactor brings together the substrate, catalysts and photons. In a real reactor, only the substrate and catalyst can be distributed uniformly. The photon distribution is always inhomogeneous due to light absorption along the path of light transmission [6]. Therefore, reactor simulation has focused on the analysis of the light distribution in order to obtain the local volumetric rate of energy absorption (LVREA). The LVREA can then be used to evaluate other reactor parameters such as the intrinsic kinetics, photonic efficiency and optimum catalyst loading [7, 8]. The light distribution is normally simulated by solving the radiation transfer equation (RTE) in the reactor space. Since this is an integro-differential equation, solving it using analytical methods is not possible [5]. Instead, the RTE is usually solved using numerical methods such as the Monte Carlo, discrete ordinates, six-flux and P1 methods. Of these methods, the stochastic Monte Carlo method has been preferred by several researchers [1] due to its rigour, flexibility and accuracy. In the Monte Carlo method, a statistically adequate number of photons are tracked from the light source until they are either absorbed by the catalyst or go beyond the reactor boundaries. In this manner, the light distribution in the reactor can be established. The light distribution in a UV lamp illuminated reactor has been evaluated extensively [8]. Several studies have also reported the light distribution in solar illuminated reactors [9, 10, 11]. Orozco et al. [3] also simulated the light

John Kabuba is with the Department of Chemical and Metallurgical Engineering, Vaal University of Technology, Vanderbijlpark, South Africa

https://doi.org/10.17758/IICBE6.C1124197

distribution in their box-type hybrid light reactor. However, according to the authors' knowledge, the light distribution in an annular-type hybrid solar/UV lamp reactor has not been reported. Since the photocatalysis reaction rate depends on the light source [12], an analysis of the light distribution in a reactor illuminated by different light sources would not be very meaningful. Another parameter, the local reaction rate (LRR), derived from the light distribution, would be much more appropriate for reactor design and optimization. Only a few studies have reported the LRR in photocatalytic reactors [13]. In this work, previously validated Monte Carlo methods for the reactor illuminated by a UV lamp and sunlight were merged and then employed for the simulation of light distribution in the hybrid light reactor. Reaction parameters for the reactor under solar and UV lamp illumination were determined from the volumetric rate of energy absorption (VREA) and phenol photocatalysis reaction rate data. The simulated LVREA and reaction parameters were then used to establish the local reaction rate (LRR) profiles in the reactor under UV lamp, solar and hybrid light illumination. Finally, the optimum catalyst loading, based on the light absorption and LRR distribution, were determined for different reactor configurations. The aim of this work was to determine the effect of reactor configuration and catalyst loading on the local reaction rate profiles.

## II. Methodology

### A. Reactor set up

The hybrid solar/UV lamp reactor in Figure 1 was illuminated internally by a 15 W black light UV lamp which was protected from the liquid using a borosilicate glass lamp sleeve. A similar borosilicate glass was used to construct the reactor wall to let in sunlight. This type of glass had a high transmittance to both solar and long wave UV light. During experiments, the reactor was set up on a roof top with a clear view to the sun. The reactor was operated in batch mode for the catalyst slurry with compressed air being used to fluidize the catalyst. Solar intensity was measured using a calibrated spectroradiometer (Stellarnet, Black Comet SR) system. This consisted of a radiation sensor (CR2 cosine receptor) which was connected to the spectroradiometer via a fibre-optic cable. The radiation data from the spectoradiometer was analysed using spectrawiz software on a computer. A special bracket enabled the radiation sensor to be positioned vertically and horizontally to measure the global horizontal UV irradiance and the global tilt UV irradiance, respectively.

### B. Monte Carlo method

The light distribution in the hybrid light reactor was simulated stochastically using a combination of the Monte Carlo methods developed previously for the reactor illuminated by the UV lamp and sunlight. In the hybrid light reactor, the photon can originate from the UV lamp or sunlight. Consequently, the source of the photon was determined as:

$$\frac{G_{UV}}{G_{UV}+G_{iN}} > R_1 \quad (1)$$

where $G_{UV}$ is the UV lamp intensity measured at the lamp surface while $G_{i,N}$ is the normal incident solar irradiance which was determined using the correlations reported previously. $R_1$ is a random number uniformly distributed between 0 and 1.

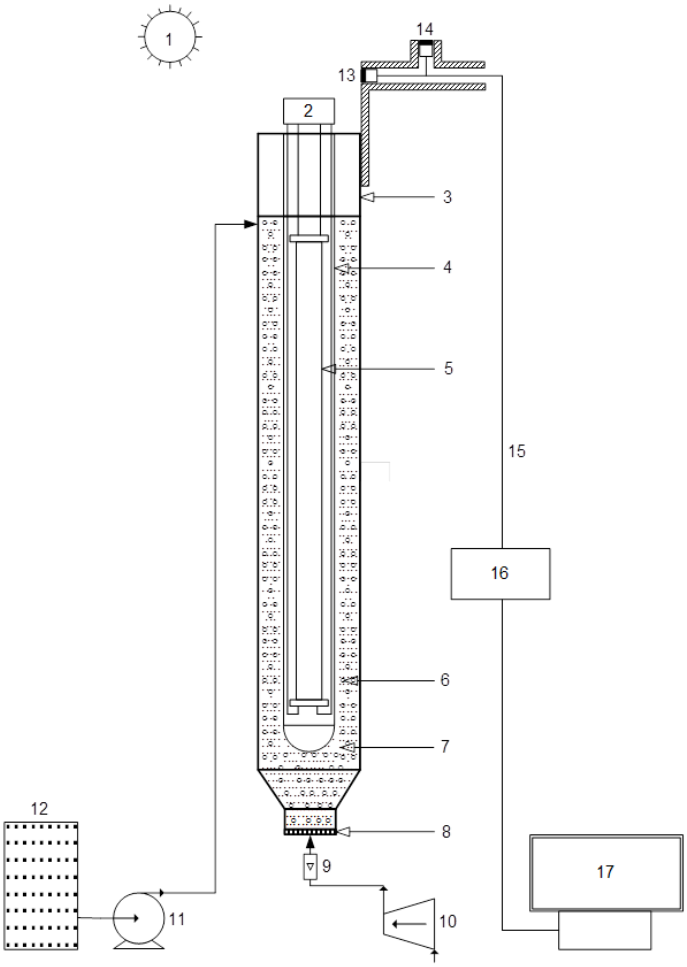


Fig. 1 Hybrid solar/UV lamp reactor (1) sun, (2) lamp power supply, (3) reactor wall, (4) lamp sleeve, (5) black light lamp, (6) air bubble, (7) catalysts particle, (8) porous distributor, (9) air rotameter, (10) air compressor, (11) peristaltic pump, (12) feed tank, (13) GTI sensor, (14) GHI sensor, (15) fibre optic cable, (16) spectroradiometer, (17) computer

TABLE I
MONTE CARLO SIMULATION PARAMETERS AND VALUES

| Parameter | Simulation values |
|---|---|
| Reactor wall | ID: 60.6 mm, OD: 65 mm, Height: 600 mm, Absorbance: 8% |
| Lamp sleeve | ID: 31.2 mm, OD: 34 mm, Height: 600 mm, Absorbance: 5.1% |
| Black light lamp | OD: 26 mm, Height: 600 mm |
| Refractive indices | Air: 1.00029, Glass: 1.473, Water: 1.332986 |
| HG asymmetric factor | UV lamp: 0.84 solar: 0.87 |

https://doi.org/10.17758/IICBE6.C1124197

If Equation (1) was evaluated as true, the photon originated from the UV lamp and its flight through the reactor was tracked using the Monte Carlo algorithm for the UV lamp illuminated reactor. However, if Equation (1) was evaluated as false, the photon was a solar photon and its flight through the reactor was described using the algorithm for the solar illuminated reactor. The photon flight through the reactor continued until the photon was either absorbed by the catalyst, lamp sleeve, wall or went beyond the reactor boundaries.

The reactor volume was divided into 11,520 cells consisting of 16 radial, 36 angular and 20 axial regions. Two identical local volumetric rate of energy absorption (LVREA) grids were employed; one to store the energy of solar photons and the other for UV lamp photons. If the photon was absorbed by the catalyst, its energy was stored in one of the two LVREA grids depending on its identity and location. The LVREA at a certain grid cell was then determined as the sum of the energy of all photons absorbed at that grid cell per unit volume of the cell [1]. The volumetric rate of energy absorption (VREA) for each of the two energy storage grids was then calculated as the sum of the LVREA in all the grid cells as:

$$VREA_{sol} = \frac{1}{V} \int LVREA_{sol} dV \quad (2)$$

$$VREA_{UV} = \frac{1}{V} \int LVREA_{UV} dV \quad (3)$$

where V is the reactor volume and the subscripts sol and UV refer to solar and UV lamp photons, respectively.

Photocatalysis is normally used to treat diluted wastewater streams in which the substrate concentration is in the order of a few mM. Therefore, photocatalysis reaction can be assumed to follow the pseudo-first order kinetics:

$$r = -\frac{dC}{dt} = k_{app} C \quad (4)$$

where r is the rate of reaction, C is the substrate concentration at time t and $k_{app}$ is the apparent first order rate constant. The effect of light intensity on the rate constant can be expressed using a power law dependence on the VREA [7] as:

$$k_{app} = k_{int}\ VREA \quad (5)$$

where $k_{int}$ is the intrinsic rate constant and α is the reaction order with respect to the VREA. Since solar and UV lamp photons were considered separately, Equation (5) can also be written as:

$$k_{app} = k_{int\_sol}(VREA_{sol})^{\alpha\_sol} + k_{int\_UV}(VREA_{UV})^{\alpha\_UV} \quad (6)$$

where the suffixes sol and UV refer to solar and UV lamp photons, respectively. The local reaction rate (LRR) was established using another grid of similar dimensions to the LVREA grids. The LRR in each of the grid cells was determined using an equation derived from Equations (4 – 6) as:

$$L_{RR} = [k_{int\_sol}(LVRE_{sol})^{\alpha\_sol} + k_{int\_UV}(LVREA_{UV})^{\alpha\_UV}]C \quad (7)$$

Some of the key Monte Carlo simulation parameters such as the reactor dimensions, refractive indices and the Henyey-Greenstein asymmetric factors are listed in Table I. The Monte Carlo algorithm for the photon flight through the hybrid light reactor is illustrated in Figure 2. Figure 3 is a cross section of the hybrid light reactor illustrating the photon flight from the lamp or the sun through the reactor. During reactor operation, catalyst particles were fluidized using air bubbles. However, photon-bubble interactions were not considered in the simulation since it had been shown previously that bubbles do not have a significant effect on the light absorption under both solar and UV lamp illumination. The Monte Carlo method was also used to establish the light distribution in simplified reactors which were illuminated by either sunlight or the UV lamp.

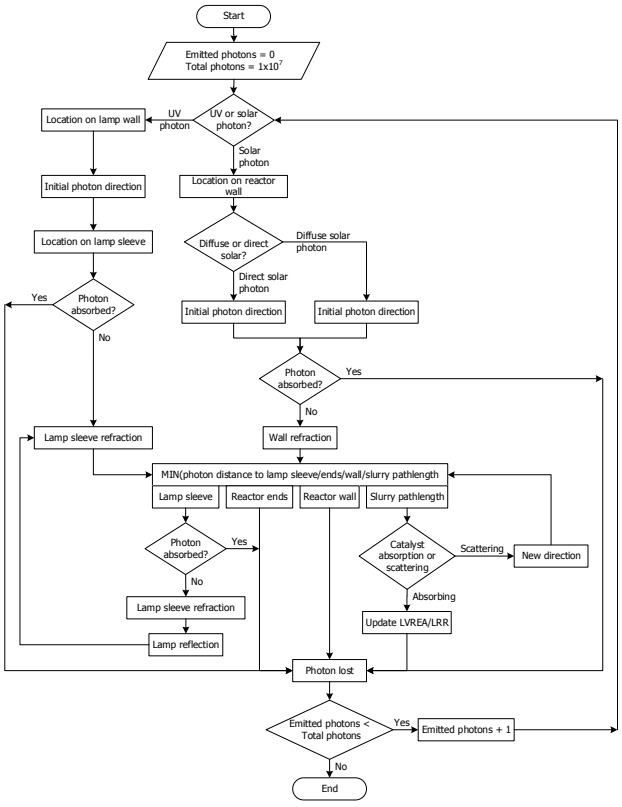


Fig. 2 Monte Carlo algorithm flow sheet

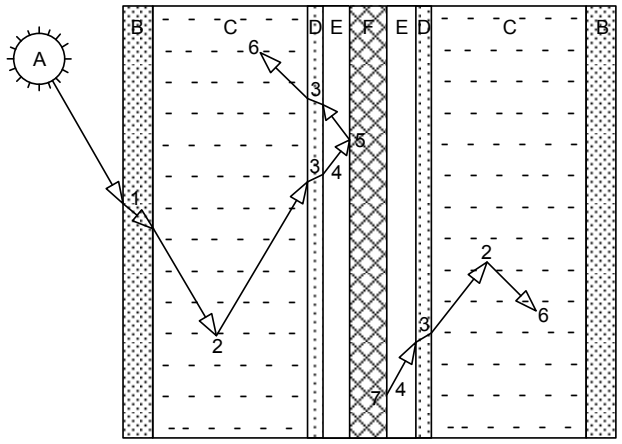


Fig. 3: Photon flight in the hybrid light reactor (1) reactor wall refraction, (2) slurry scattering, (3) lamp sleeve refraction, (4) air gap photon flight, (5) lamp wall reflection, (6) catalyst absorption, (7) UV lamp photon emission. (A) solar position, (B) reactor wall, (C) catalyst slurry, (D) lamp sleeve, (E) air gap, (F) UV lamp

### *B. Photocatalysis Experiments*

During photocatalysis experiments, three different reactor configurations were employed based on the type of illumination. The annular UV lamp and annular solar reactors were illuminated by the UV lamp and sunlight, respectively while the hybrid light reactor was illuminated by both light sources. Photocatalysis experiments were carried out at different catalyst loadings in each of these reactor configurations. First, the reactor was covered with a black canvas to shut off sunlight. Then, the reactor was filled with 1250 mL phenol solution with a concentration of 50 mg/L and a measured amount of catalyst loading between 0.25 g/L and 0.6 g/L. The catalyst slurry solution was kept under mixing in the dark for 30 minutes to ensure adsorption-desorption equilibrium. At the same time, the UV lamp was switched on and left to warm for 30 minutes outside the reactor. For the annular UV lamp reactor, the lamp was inserted into the reactor lamp sleeve to start the reaction. In case of the annular solar reactor, the canvas covering the reactor was removed to expose the reactor to sunlight and start the photocatalysis reaction. For the hybrid light reactor, the reaction was started by simultaneously inserting the lamp into the lamp sleeve and removing the canvas to illuminate the reactor with both the UV lamp and sunlight. The substrate solution was sampled every 10 minutes, filtered with a 0.45 µm nylon syringe filter to remove the catalyst. Then, the concentration of the phenol solution was analysed using a Perkin-Elmer high performance liquid chromatography (HPLC). The HPLC was equipped with a C18 column (Perkin-Elmer) and a diode array detector (DAD) set at a wavelength of 270 nm. The mobile phase consisted of HPLC grade acetonitrile and water at a ratio of 60:40 and a flow rate of 1 mL/min. During substrate sampling, the global horizontal UV irradiance and the global tilt UV irradiance were recorded. An average of these values was used to compute the normal solar intensity incident upon the reactor during the photocatalysis experiment using the correlations reported previously. The intensity of the light incident upon the reactor boundaries and the solar conditions during the experiments in the different reactor configurations are listed in Table II:

TABLE II
LIGHT INTENSITY OF DIFFERENT REACTOR CONFIGURATIONS

| Reactor configuration | Light intensity (mol/s) | Solar zenith angle (°C) | Solar diffuse fraction |
|---|---|---|---|
| Annular UV lamp | $2.159\text{x}10^{-5}$ | | |
| Annular solar | $9.035\text{X}10^{-6}$ | 21.8 | 0.153 |
| Hybrid solar/UV lamp | 2.159x10-5 (UV lamp) $7.670\text{x}10^{-6}$ (solar) | 29.5 | 0.337 |

## III. RESULTS AND DISCUSSION

### *A. Reaction rate parameters*

The value of α and $k_{int}$ are usually determined by fitting VREA to experimentally determined values of $k_{app}$ [7]. This is carried out by plotting $k_{app}$ and VREA on a log-log scale from which the values of $k_{int}$ and α can easily be determined from the intercept and slope, respectively. In this work, experimental values of kapp were determined from the photocatalysis of phenol at different catalyst loadings in the annular UV lamp and annular solar reactors. The values of the VREA were determined from Monte Carlo simulation of the light distribution in those same reactor configurations. The simulations were carried out at the experimental catalyst loading and the intensity of the UV lamp/sunlight at the time of the experiments. The plots of $k_{app}$ vs VREA in the annular UV lamp and annular solar reactors are shown in Figure 4. Under UV lamp illumination, α and $k_{int}$ were found to be 0.75 and $1.94\times10^{-5}$ $cm^{2.25}$ µW-0.75 $min^{-1}$, respectively. The value of α is close to the value of 0.82 reported by [7] for an annular UV lamp reactor containing P25 $TiO_2$ catalyst irradiated with an 8W black light lamp. The values of α and $k_{int}$ under solar illumination were found to be 0.74 and $2.55\times10^{-5}$ $cm^{2.22}$ µW-0.74 $min^{-1}$, respectively. The value of α usually lies between 0.5 and 1. At low values of VREA, very little electron-hole recombination occurs; therefore, most of the absorbed radiation results in reaction. In this situation, the value of α approximates 1. As the value of VREA increases, the rate of electron-hole generation outstrips the rate of photocatalysis resulting in electron-hole recombination. This decreases the value of α to 0.5 [7]. A value of α between 0.5 and 1 is common in optically thick reactors in which both first order and half order regimes exist in the same reactor [5]. For both the annular solar and UV lamp reactors, the value of α was between 0.5 and 1, which shows that both first order and half order regimes were present in the reactor. It is conceivable that the region near the light source had half order reaction

https://doi.org/10.17758/IICBE6.C1124197

which increased to first order reaction further away from the light sources [5]. The value of α under solar illumination was slightly lower than the corresponding value under UV lamp illumination. This can be attributed to the presence of high energy photons in the 300 – 345 nm wavelength range in the solar spectrum which were not present in the UV lamp spectrum (Figure 5). These high energy photons could generate much more electrons and holes resulting in a higher rate of electron-hole recombination under solar illumination as compared to UV lamp illumination.

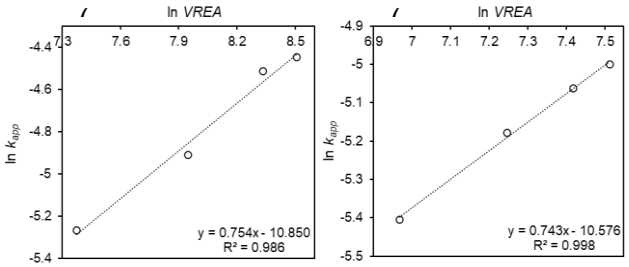


Fig. 4 Mapping nonlinear data to a higher dimensional feature space

Generally, the reaction rate under UV lamp illumination was higher than that under solar illumination. For example, at a catalyst loading of 0.2 g/L, the reaction rate under UV lamp and solar illumination was 0.548 and 0.337 mg $L^{-1}$ $min^{-1}$, respectively (Figure 6). This could be attributed to two factors. First, the intensity of the UV lamp was higher than that of sunlight (Table I). This resulted in higher values of the VREA and reaction rate under UV lamp illumination. Secondly, as shown by the respective values of α, the efficiency of conversion of the absorbed UV lamp photons into viable electron-hole pairs was better than that of solar photons, and this resulted in a higher reaction rate. Other studies have also found that the rate of photocatalysis depends on the type of light source [7, 12].

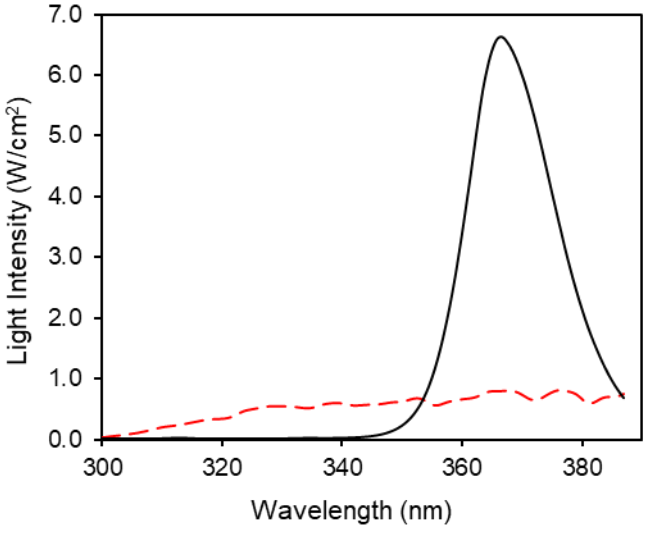


Fig. 5 Light spectra of sunlight (– – –) and UV lamp (——) between 300 and 387 nm

The reaction rate under both light sources was generally higher than the reaction rate under either solar or UV lamp illumination. This was mainly attributed to the dual illumination of the reactor from both the inside and outside which minimized dark zones and improved overall catalyst activation. It should be noted that the sum of the reaction rate under solar and UV lamp illumination did not equal the reaction rate under dual illumination. For example, at a catalyst loading of 0.2 g/L, the sum of the reaction rate under UV lamp and solar illumination was 0.885 mgL-1min-1 while that under hybrid light illumination was 0.788 mgL-1min-1. This discrepancy was due to the fact that the solar and hybrid light photocatalysis experiments were carried out on different days with different solar intensities.

Figure 6 shows a very good fit between the experimental and simulated reaction rate under UV lamp, solar and hybrid light illumination. The good fit of the simulated reaction rate under UV lamp and solar illumination was expected since the simulated rate profiles were evaluated from experimental data. The reaction parameters (α and $k_{int}$) obtained under UV lamp and solar illumination were used to determine the simulated reaction rate profiles under hybrid light illumination without any other adjustable parameters. The good fit between the experimental and simulated reaction rate under hybrid light illumination shows the accuracy and reliability of Monte Carlo simulation.

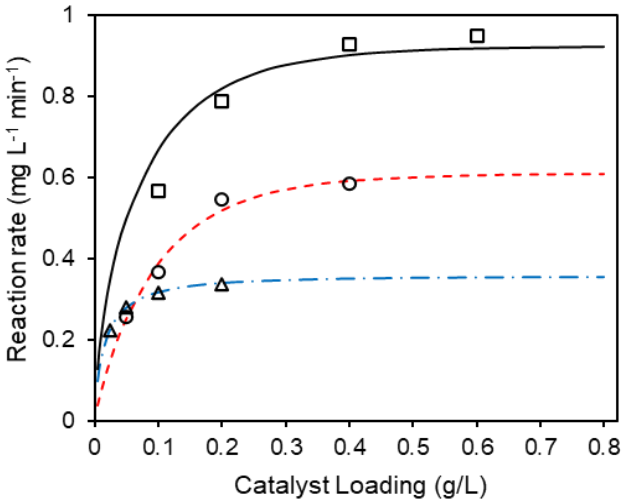


Fig. 6 Experimental and simulated rate of phenol photocatalysis under different light sources. Solar-simulated (— · —), solar-experimental (Δ), UV lamp-simulated (— — —), UV lamp-experimental (○), hybrid-simulated (——), hybrid-experimental (□).

### *B. Local reaction rate profiles*

After evaluating the intrinsic reaction rate constants ($k_{int}$) and the reaction order with respect to the VREA (α), these values were used to determine the local reaction rate (LRR) profiles in the reactor. Previous studies had shown that changes in the light absorption were insignificant along the axial axis in this reactor under both solar and UV lamp illumination. Therefore, LRR profiles were only investigated

https://doi.org/10.17758/IICBE6.C1124197

on the radial plane. LRR profiles at three catalyst loadings (0.25, 1.0 and 4.0 g/L) in four reactor configurations (tubular solar, annular solar, annular UV lamp and hybrid light) were analysed using polar plots across the reactor centre-line (z = 300 mm) (Figure 7a – l).

The LRR values were presented on a dimensionless scale with the maximum LRR indicated on each sub-figure. The tubular and annular solar reactors were illuminated from the right side of the polar plots while the annular UV lamp reactor was illuminated internally. The hybrid light reactor was illuminated from the right side of the polar plot by sunlight and also internally by the UV lamp. To facilitate comparison among the different reactor configurations, Monte Carlo simulations were carried out using the same set of light intensity values measured during the hybrid light experiments (Table II). A pair of 2D plots were also used to show the radial LRR profiles across the polar plots. The radial LRR profiles for the tubular and annular

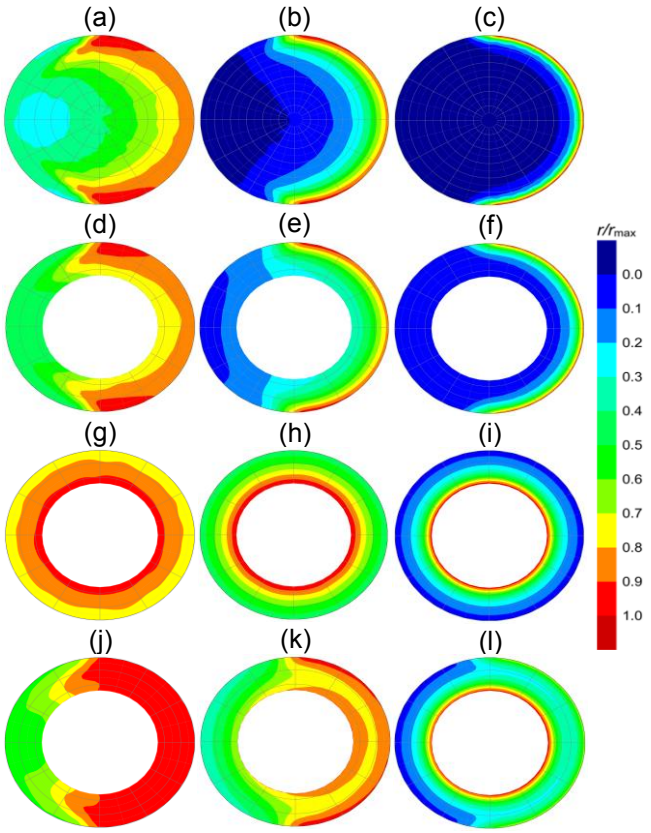


Fig. 7 Local reaction rate for different reactors and catalyst loadings. (a) Tubular solar-0.025 g/L (b) Tubular solar-0.1 g/L (c) Tubular solar-0.4 g/L (d) Annular solar-0.025 g/L (e) Annular solar-0.1 g/L (f) Annular solar-0.4 g/L (g) Annular UV lamp-0.025 g/L (h) Annular UV lamp-0.1 g/L (i) Annular solar-0.4 g/L (j) Hybrid-0.025 g/L (k) Hybrid-0.1 g/L (l) Hybrid-0.4 g/L

solar reactors were presented in Figure 8a while those for the UV lamp and hybrid light illuminated reactors were shown in Figure 8b.

In the solar and UV lamp illuminated reactors (Figure 7a – i), the LRR decreased from the illuminated side of the reactor to the unilluminated side. The radial profiles showed an exponential decay of the LRR along the light path with the gradient of the decay increasing with an increase in the catalyst loading (Figure 8a, b). At the lowest catalyst loading (0.025 g/L), a fairly uniform but low LRR profile was observed in the reactor. For example, in the tubular solar reactor, the radial LRR ranged from 0.106 to 0.245 mgL-1min-1 at 0.025 g/L catalyst loading (Figure 8a). At the highest catalyst loading (0.4 g/L), very high values of the LRR were observed near the illuminated region with most of the reactor exhibiting very low LRR values. For example, at a catalyst loading of 0.4 g/L, the radial LRR dropped from 1.324 $mgL^{-1}min^{-1}$ at the illuminated wall to 0.002 $mgL^{-1}min^{-1}$ at the unilluminated wall of the tubular solar reactor (Figure 8a). The exponential decay in the LRR was due to light attenuation along the light path due to catalyst absorption and scattering. An increase in the catalyst loading has been observed to increase the light attenuation [1], and this increased the decay of the LRR along the light path.

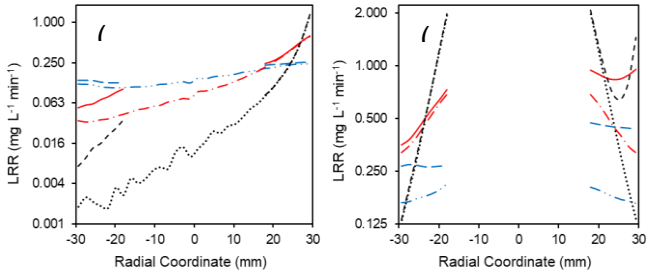


Fig. 8 Radial LRR profiles (a) Tubular solar-0.025 g/L (— · · —), Tubular solar-0.1 g/L (— · —), Tubular solar-0.4 g/L (·····), Annular solar-0.025 g/L (— — —), Annular solar-0.1 g/L (——), Annular solar-0.4 g/L (- - -); (b) Annular UV-0.025 g/L (— · · —) Annular UV-0.1 g/L (— · —) Annular UV-0.4 g/L (·····) Hybrid-0.025 g/L (— — —) Hybrid-0.1 g/L (——) Hybrid-0.4 g/L (- - -).

The radial LRR profiles showed that the annular solar reactor had a better LRR distribution than the tubular solar reactor. Whilst the LRR profiles near the illuminated wall were similar for both solar reactors, the LRR values near the unilluminated wall was higher in the annular reactor at all catalyst loadings. For example, at a catalyst loading of 0.4 g/L, the radial LRR ranged from 0.002 to 1.324 $mgL^{-1}min^{-1}$ in the tubular reactor and from 0.007 to 1.324 $mgL^{-1}min^{-1}$ in the annular reactor (Figure 8a). Light absorption by catalyst particles at the centre of the tubular reactor reduced the amount of light reaching the unilluminated region. In contrast, the centre of the annular reactor was filled with air which did not absorb any light, and this increased the incident light reaching the unilluminated region. The good light utilization in the annular configuration provided a platform for even better light utilization in the hybrid light reactor.

Generally, higher LRR values were observed in the annular UV lamp reactor as compared to the solar illuminated reactors. For example, at a catalyst loading of 0.1 g/L, the

https://doi.org/10.17758/IICBE6.C1124197

minimum radial LRR values were 0.053 and 0.318 $mgL^{-1}min^{-1}$ in the annular solar and UV lamp reactors, respectively (Figure 8a, b). This was due to the higher intensity and better catalyst utilization of UV lamp photons as compared to solar photons. Deeper penetration of UV lamp photons would be advantageous for hybrid light operation as this would provide good illumination to the solar dark zone, the side of the reactor that was not illuminated by sunlight. In the hybrid light reactor, the LRR in the solar illuminated zone was strongly influenced by the two light sources. At low catalyst loading (0.025 g/L), a fairly uniform LRR was observed in this zone (Figure 7j). At this low catalyst loading, both solar and UV lamp photons could penetrate deep into the catalyst slurry, resulting in the illumination of all catalysts by both light sources. As the catalyst loading increased, the highest LRR values were restricted to a narrow region near the solar illuminated wall and the lamp sleeve (Figure 7k – l). This was characterized by the U-shaped curve of the radial LRR in the solar illuminated zone which became very steep at the highest catalyst loading (Figure 8b). This trend was attributed to an increase in the light attenuation with catalyst loading which reduced the path length of light in the reactor (Moreira et al., 2010). As a result, most of the light was absorbed in the region near both light sources resulting in high LRR in these regions.

It can also be observed from Figure 7l that the reaction rate near the lamp sleeve was markedly higher than that near the solar-illuminated wall. At such high catalyst loadings, rapid light attenuation ensured that the reaction rate near the boundaries was due to a specific light source. As compared to sunlight, light from the UV lamp had a higher intensity and reaction order with respect to the VREA. As a result, the more numerous UV lamp photons were also more likely to form electron-hole pairs in the catalysts, and this resulted in a higher LRR near the lamp sleeve. The lowest LRR in the hybrid light reactor was observed in the solar dark zone (Figure 7j – l). For example, at a catalyst loading of 0.1 g/L, the lowest radial LRR was 0.834 $mgL^{-1}min^{-1}$ in the solar illuminated zone and 0.353 $mgL^{-1}min^{-1}$ in the solar dark zone (Figure 8b). This was due to the fact that the solar dark zone was not directly illuminated by sunlight and the solar photons from the solar illuminated zone were blocked by the catalyst and UV lamp. The solar photons reaching the solar dark zone decreased with an increase in catalyst loading. At the highest catalyst loading, very little solar photons could reach the dark zone; consequently, most of the illumination in the solar dark zone was provided by the UV lamp. This is clearly evident from the radial LRR profiles in the solar dark zone at a catalyst loading of 0.4 g/L which shows similar LRR profiles in the annular UV lamp and hybrid light reactors (Figure 8b).

### *C. Optimum Catalyst loading*

Catalyst loading is one of the most critical parameters in evaluating the performance of a photoreactor since it affects hydrodynamics, irradiation and mass transfer and reaction kinetics. The optimum catalyst loading was investigated from the simulated reaction rate in the four reactor configurations (Figure 9a). For all reactor configurations, increasing the catalyst loading resulted in an increase in the overall reaction rate up to an optimal value beyond which any further increase in the catalyst loading resulted in only a marginal increase in the reaction rate. In this respect, the optimum catalyst loading in the tubular solar, annular solar, annular UV lamp and hybrid light reactors were found to be 0.15, 0.2, 0.4, and 0.4 g/L, respectively (Figure 9a). It should be noted that similar values were obtained using the VREA data in the tubular solar reactor and annular UV lamp reactor. This further proves the hypothesis that VREA data can be used to predict the optimum catalyst loading without the need for photocatalysis experiments. From the simulation studies, it was observed that the optimum catalyst loading in the annular solar reactor was higher than that in the tubular solar reactor. This can be attributed to better penetration of solar photons in the annular solar reactor. Also, the annular UV lamp reactor had a higher optimum catalyst loading as compared to the solar reactors. This was due to the higher light output from the UV lamp as compared to sunlight. The optimum catalyst loading in the annular UV lamp and hybrid light reactors were equal. In the hybrid light reactor, the influence of the UV lamp was much stronger than that of sunlight since UV lamp photons could penetrate deeper into the catalyst slurry. Therefore, the optimum catalyst loading was predominantly determined by the pathlength of UV lamp photons which explains the similar optimum catalyst loading in the two reactor configurations. In a photocatalytic reactor, an increase in the catalyst loading has been observed to increase the overall light absorption and decrease the light distribution [1]. The conventional method of evaluating the optimum catalyst loading using the reaction rate or VREA, therefore, yields a value that maximizes the overall reaction rate or light absorption without reference to the light distribution and catalyst utilization. At this optimum catalyst loading, it is often the case that a lot of the catalyst in the reactor are poorly irradiated and therefore wasted. This could present an opportunity for further optimization in cases where the cost of the catalyst far exceeds the photon cost. In such a situation, it would be necessary to consider the optimum catalyst loading with respect to the light distribution or the LRR distribution. Recently, Acosta-Herazo et al. [9] proposed a new parameter, the energy absorption distribution index (EADI), which could be used to evaluate the highest catalyst loading that would ensure the best possible light distribution. The EADI was evaluated as:

$$EADI = \frac{VREA}{RSD_{LVREA}} \tag{8}$$

where the RSDVREA is the relative standard deviation of the local volumetric rate of energy absorption (LVREA). In this work, an analogous parameter, the reaction rate distribution index (RRDI) is proposed. The RRDI is based on the LRR and is computed as:

$$RRDI = \frac{r}{RSD_{LRR}} \tag{9}$$

where r is the overall reaction rate and RSDLRR is the relative standard deviation of the LRR.

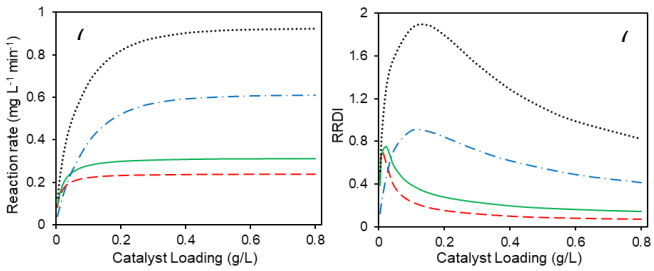


Fig. 9: Effect of catalyst loading on the (a) overall reaction rate (b) RRDI in different reactor configurations. Tubular solar (— — —), Annular solar (——), Annular UV lamp (— · —), Hybrid light (·····)

## IV. Conclusion

In this study, previously developed Monte Carlo models were adapted for simulation of the light distribution in a hybrid solar/UV lamp photocatalytic reactor. The reaction order with respect to the VREA was found to be 0.75 and 0.74 under UV lamp and solar illumination, respectively. The reaction rate under both light sources was generally higher than that under either solar or UV lamp illumination. A good fit between simulated and experimental reaction rate under hybrid light illumination was obtained which highlighted the accuracy of Monte Carlo simulation.

The optimum catalyst loading, based on the overall reaction rate, was found to be 0.15 mg/L (tubular solar), 0.2 mg/L (annular solar), 0.4 mg/L (annular UV), and 0.4 g/L (hybrid) in the tubular solar, annular solar, annular UV lamp and hybrid light reactors, respectively. Using the reaction rate distribution index (RRDI), the optimum catalyst loading, based on the reaction rate distribution was found to be 0.01, 0.025, 0.1 and 0.15 g/L in the four reactor configurations. The radial reaction rate profiles showed a non-uniform distribution of the reaction rate which worsened with an increase in catalyst loading. In the hybrid light reactor, the regions nearest to the light sources had the highest reaction rate while the solar dark side had the lowest reaction rate. The local reaction rate (LRR) profiles and the RRDI in the different reactors revealed that the LRR distribution followed the order: hybrid light > annular UV lamp > annular solar > tubular solar reactors. The RRDI also showed a drastic improvement in the LRR distribution due to hybrid light illumination. This study highlighted the accuracy and reliability of the Monte Carlo method for simulating the reaction rate profiles in a hybrid solar/UV lamp reactor.

## Conflicts of Interest

I declare no conflict of interest.

## References

[1] P.J. Valades-Pelayo, J. Moreira, B. Serrano & H. De Lasa, "Boundary conditions and phase functions in a photo-crec water-II reactor radiation field". *Chem. Eng. Sc*., vol. 107, pp. 123–136, 2014. https://doi.org/10.1016/j.ces.2013.12.013

[2] R. A. R. Monteiro., C. Rodrigues-Silva, F.V.S. Lopes, A.M.T. Silva, R.A.R. Boaventura & V.J.P. Vilar, "Evaluation of a solar/UV annular pilot scale reactor for 24h continuous photocatalytic oxidation of n-decane". *Chem. Eng. J*., vol. 280, pp. 409–416, 2015 https://doi.org/10.1016/j.cej.2015.06.014

[3] S.L. Orozco, C.A. Arancibia-Bulnes & R. Suárez-Parra, "Radiation absorption and degradation of an azo dye in a hybrid photocatalytic reactor". *Chem. Eng. Sc*., vol. 64(9), pp. 2173–2185, 2009 https://doi.org/10.1016/j.ces.2009.01.038

[4] A. Durán, J.M. Monteagudo, I. San Martín & S. Merino, "Photocatalytic degradation of aniline using an autonomous rotating drum reactor with both solar and UV-C artificial radiation". *J. Environ. Man*., 210, pp.122–130, 2018. https://doi.org/10.1016/j.jenvman.2018.01.012

[5] Y. Boyjoo, M. Ang & V. Pareek. "Some aspects of photocatalytic reactor modeling using computational fluid dynamics". *Chem. Eng. Sci.,* vol. 101, pp. 764–784, 2013. https://doi.org/10.1016/j.ces.2013.06.035

[6] G. Camera-Roda, V. Augugliaro, A.G. Cardillo, V. Loddo, L. Palmisano, F. Parrino & F. Santarelli. "A reaction engineering approach to kinetic analysis of photocatalytic reactions in slurry systems". *Catalysis Today,* vol. 259, pp. 87–96, 2016. https://doi.org/10.1016/j.cattod.2015.05.007

[7] G. Li Puma, V. Puddu, H.K. Tsang, A. Gora & B. Toepfer. "Photocatalytic oxidation of multicomponent mixtures of estrogens (estrone (E1), 17β-estradiol (E2), 17α-ethynylestradiol (EE2) and estriol (E3)) under UVA and UVC radiation: Photon absorption, quantum yields and rate constants independent of photon absorp". *Appl. Catalysis B: Environ*., vol. 99(3–4), pp. 388–397, 2010. https://doi.org/10.1016/j.apcatb.2010.05.015

[8] J. Moreira, B. Serrano, A. Ortiz & H. de Lasa. "Evaluation of photon absorption in an aqueous $TiO_2$ slurry reactor using Monte Carlo simulations and macroscopic balance". *Ind. & Eng. Chem. Res*., vol. 49(21), pp.10524–10534, 2020. https://doi.org/10.1021/ie100374f

[9] R. Acosta-Herazo, P.J. Valadés-Pelayo, M.A. Mueses, M.H. Pinzón-Cárdenas, C. Arancibia-Bulnes & F. Machuca-Martínez. "An optical and energy absorption analysis of the solar compound parabolic collector photoreactor (CPCP): The impact of the radiation distribution on its optimization". *Chem. Eng. J*., vol. 395, 125065, 2020. https://doi.org/10.1016/j.cej.2020.125065

[10] J. Hou, Q. Wei, Y. Yang & L. Zhao. "Experimental evaluation of scattering phase function and optimization of radiation absorption in solar photocatalytic reactors". *Appl. Therm. Eng*., vol.127, pp.302–311, 2017. https://doi.org/10.1016/j.applthermaleng.2017.08.046

[11] K.S. Ochoa-Gutiérrez, E. Tabares-Aguilar, M.A. Mueses, F. Machuca-Martínez & G. Li Puma. "A Novel Prototype Offset Multi Tubular Photoreactor (OMTP) for solar photocatalytic degradation of water contaminants". *Chem. Eng. J*., vol.341, pp.628–638, 2018. https://doi.org/10.1016/j.cej.2018.02.068

[12] C.G. Joseph, Y.H. Taufiq-Yap, G. Li Puma, K. Sanmugam & K.S. Quek. « Photocatalytic degradation of cationic dye simulated wastewater using four radiation sources, UVA, UVB, UVC and solar lamp of identical power output". Desalination and Water Treatment, vol.57(17), pp. 7976–7987, 2016. https://doi.org/10.1080/19443994.2015.1063463

[13] Y. Boyjoo, M. Ang & V. Pareek. "CFD simulation of a pilot scale slurry photocatalytic reactor and design of multiple-lamp reactors". *Chem. Eng. Sci*., vol.111, pp. 266–277, 2014. https://doi.org/10.1016/j.ces.2014.02.022

**John Kabuba** is a Professor and Faculty Research Ethics Chairperson in the Faculty of Engineering and Technology, Vaal University Technology. He has more than 19 years' experience in academia which he gained at University of Johannesburg and Vaal University of Technology. He is a recipient of several awards and scholarships for academic excellence. He has an extensive track

record in human capacity development having supervised 112 Bachelor’s, 12 Master’s and 3 Doctoral students to completion. He has published more than 92 international peer reviewed and refereed scientific articles in journals, conferences, book chapters and book. Regularly servers as an external examiner for Masters dissertations and PhD theses as well as a peer reviewer for ISI journals. His research interests are mainly in the broad areas of Wastewater treatment, Hydrometallurgy and Neural Network Applications.

https://doi.org/10.17758/IICBE6.C1124197